De novo characterization of *Platycladus orientalis* transcriptome and analysis of its gene expression during aging

Ermei Chang[1]*, Xiamei Yao[1,2]*, Jin Zhang[1], Nan Deng[1], Zeping Jiang[1§], Shengqing Shi[1§]

[1]State Key Laboratory of Tree Genetics and Breeding, Key Laboratory of Tree Breeding and Cultivation of State Forestry Administration, Research Institute of Forestry, Chinese Academy of Forestry, Beijing, China.

[2]School of Biological Science and Food Engineering, Fuyang Normal University, Fuyang, Anhui, China

*Co-first author.

[§]Correspondence:

Dr. Shengqing Shi

Chinese Academy of Forestry

Research Institute of Forestry

State Key Laboratory of Tree Genetics and Breeding

No. 1 Dongxiaofu, Xiangshan Road

Haidian, Beijing, 100091, China

shi.shengqing@caf.ac.cn

Dr. Zeping Jiang

Chinese Academy of Forestry

Research Institute of Forestry

State Key Laboratory of Tree Genetics and Breeding

No. 1 Dongxiaofu, Xiangshan Road

Haidian, Beijing, 100091, China

jiangzp@caf.ac.cn

PeerJ Preprints | https://doi.org/10.7287/peerj.preprints.2866v1 | CC BY 4.0 Open Access | rec: 10 Mar 2017, publ: 10 Mar 2017

ABSTRACT

Platycladus orientalis in China has a lifespan of one to several thousands of years. The long lifespans of trees have attracted interest in aging at the molecular level. There is little information on how the global process is controlled. In this study, the MDA content, SOD and POD activities were higher in ancient trees than in 20-year-old *P. orientalis*, and the content of soluble protein showed the inverse trend. We obtained 48,044 unigenes having an average length of 896 bp from pooled samples of *P. orientalis* by transcriptome sequencing. Microarray analysis produced a high-resolution age-course profile of gene expression levels in different age of *P. orientalis.* In total, 418 differentially expressed genes were identified. The use of highly informative clustering revealed distinct time points at which oxidation reduction and photosynthesis pathways changed. Eight clusters with distinctive expression patterns were identified, the expression of metabolism, photosynthesis, oxidation reduction and transporters related genes were downregulated and protein synthesis, transcription, signal transduction and senescence related genes were upregulated with increasing age. Total chlorophyll, chlorophyll a, and chlorophyll b levels were decreased steadily with increasing age. This study discovery of potential candidate genes affecting photosynthesis in different *P. orientalis* ages and at senescence, and for identification of the functions of genes involved in regulation of photosynthesis. This work also suggests that improving photosynthetic efficiency under field conditions will require the consideration of multiple factors.

Subjects Evolutionary studies, Genomics, Plant science

Keywords Longevity; *Platycladus orientalis*; Senescence; Transcriptome; Photosynthesis

PeerJ Preprints | https://doi.org/10.7287/peerj.preprints.2866v1 | CC BY 4.0 Open Access | rec: 10 Mar 2017, publ: 10 Mar 2017

INTRODUCTION

Several woody perennials involved in *Sequoia sempervirens*, *Sequoiadendron giganteum* and *Pinus longaeva*, can live several hundred years or even millennia (*Munné-Bosch, 2007*). These trees can have extremely long life span with several thounsands of years, whose mechnisms about how to regulate or resist aging at physiological and molecular levels has become one of the hot focuses in plant resisting senesences (*Chang et al., 2012*; *Chang et al., 2016*). Some physiological and metabolic changes during aged have been reported in conifer (*Klimešová, 2015*; *Nemoto and Finkel, 2004*). Increases in telomere length and telomerase activity may directly/indirectly contribute to the increased life-span and longevity of *P. longaeva* (*Flanary and Kletetschka, 2005*). However, no significant age-related differences were found between bristlecone pines of 4,713 and 23 years of age (*Lanner & Connor 2001*; *Sillett et al., 2015*). Untangling the mechanisms of perennial aging has attracted significant attention in the past, but remains a matter of debate (*Peñuelas, 2005*; *Munné-Bosch, 2008*; *Issartel and Coiffard, 2011*).

Studies on physiology and genetics show that the senescence process is tightly controlled and requires massive changes at the mRNA level (*Duan et al., 2016*). Genes encoding senescence-associated receptor-like kinases (SARK and SIRK) have also been identified in bean and *Arabidopsis* (*Guo et al., 2004*). Changes in gene expression are usually mediated by changes in the activity of transcription factors including members of the NAC, WRKY, MYB, C2-H2 zinc-finger, bZIP, and AP2/EREBP families (*Andersson-Gunnerås et al., 2004*; *Breeze et al., 2011*), act as regulatory nodes between signaling branches, contributing to the fine-tuning of developmental or defense reactions (*Zhang et al., 2016*). Many genes involved in 1-Cys peroxiredoxin and Heat-shock proteins play an important role in the plant defense process (*Lim et al., 2005*; *Watson and Riha, 2011*; *Hayashi et al., 2016*; *Sun et al., 2016*; *Tillmann et al., 2016*), Calmodulin-binding protein is a positive regulator of both disease resistance and drought tolerance in *Arabidopsis*. But the causes of defense mechanism responses in *P. orientalis* require further study.

PeerJ Preprints | https://doi.org/10.7287/peerj.preprints.2866v1 | CC BY 4.0 Open Access | rec: 10 Mar 2017, publ: 10 Mar 2017

Senescence may be considered an adaptive strategy of plants to the prevailing environmental conditions that begins with catabolism of macromolecules such as chlorophyll, proteins, and ucleic acids (*Palma et al., 2006*; *Huang et al., 2010*; *Gupta et al., 2016*). The decrease in photosynthetic rates is an inevitable consequence of increased size and age in *Arabidopsis* and *Populus*(*Nemoto and Finkel, 2004*; *Keskitalo et al., 2005*; *Bond 2000*). The photosynthetic rate and the balance of forces was broken, and the transcription of related regulatory genes (*rbcL*, *rbcS*, *petB* and *psbA*) decreased sharply (*Hörtensteiner, 2009*). Photosynthesis converts light energy into chemical energy, and the electron transfer in the energy conversion process is regulated by the oxidation reduction (redox) system. Cytochrome c is an important part of the mitochondrial electron transport chain, as well as a major protein that regulates the redox status (*Gonzales and Neupert, 2000*). There is a strong relationship between oxidation reduction and lifespan (*Reich et al., 2006*). However, little is known about the relative contributions of organelles to the oxidation reduction associated with senescence in trees.

At present, gene microarray technology has been widely applied in the study of functional genomics of *Arabidopsis*, rice and other plants under stress conditions (*Wagstaff et al., 2009*; *Breeze et al., 2011*). Senescence mutants and transgenic anti-aging plants were obtained (*Bhalerao et al., 2003*; *Andersson-Gunneras et al., 2004*), and can be used to explain the nature and mechanisms of plant senescence at the molecular level. High-throughput sequencing technology enables us to combine transcriptional sequencing and digital expression profiling, allowing for the study of high-throughput gene expression profiles from non-model plants (*Tang et al., 2011*). The differential expression of genes in *P. orientalis* of different ages has not been reported, and the longevity of *P. orientalis* is regulated by many factors. Molecular biological methods will be helpful in studying the ancient trees (*Peñuelas, 2005*). In this study, transcriptome sequencing and an expression analysis of different aged *P. orientalis* (20 ± 3-, 300 ± 100-, 1,000 ± 300-, and 1,700 ± 500-year-old) was conducted using high-throughput sequencing technology. Combining the analysis of gene expression levels with physiological and biochemical data, the regulatory mechanisms of the anti-aging process of *P. orientalis* at the molecular level is discussed, laying the foundation for understanding of expression differences and specific genes related to aging.

PeerJ Preprints | https://doi.org/10.7287/peerj.preprints.2866v1 | CC BY 4.0 Open Access | rec: 10 Mar 2017, publ: 10 Mar 2017

MATERIALS AND METHODS

Plant materials

Fresh leaves were collected from the 20 ± 3-, 300 ± 100-, 1,000 ± 300-, and 1,700 ± 500-year-old (based on the records from parks) individuals of *P. orientalis* growing under similar conditions in Zhongshan Park in Beijing (N 39°54′26.37″, E 116°23′29.22″) (Fig. 1). Twenty-year-old trees (adult tree) were used as a control; other trees were considered ancient trees (each age group with three trees to provide three replicates) (*Zhang et al., 2015*). Fresh leaves collected from branches with the same exposure to light and with similar heights and diameters were selected for sampling. Furthermore, the leaves were healthy current-year leaves, and they were selected from trees without large dead branches, plant diseases, and insect pests. The sampled sun-exposed leaves were detached from the outer portions of the crowns (as much as possible under similar environmental conditions), and 5-7 g of fresh leaves was collected from each tree three times a week, at 8 am on each occasion. Leaves were flash frozen in liquid nitrogen and stored at 80°C. Samples were approved by Zhongshan Park administrative office.

Physiological Index determination

The content of total soluble protein and Malondialdehyde (MDA) were measured according to *Cui et al.,* (*2016*) and *Heath and Packer* (*1968*), respectively. The presence of SOD activity and POD activity were detected according to *Dhindsa et al.,* (*1981*). The total chlorophyll content and the amount of chlorophyll a and chlorophyll b were estimated according to *Breeze et al.,* (*2011*). Differences were scored as statistically significant at the $P < 0.05$ or $P < 0.01$ levels.

Total RNA extraction

Total RNA was isolated from the leaves of *P. orientalis* according to the protocol of the

PeerJ Preprints | https://doi.org/10.7287/peerj.preprints.2866v1 | CC BY 4.0 Open Access | rec: 10 Mar 2017, publ: 10 Mar 2017

Column Plant RNAout kit (TIANDZ, Beijing, China). Then, the quality and integrity of RNA was assayed by a NanoPhotometer® spectrophotometer (Implen, CA, USA), electrophoresis through 1.5% agarose gels and Agilent 2100 Bioanalyzer (Agilent Technologies, Santa Clara, CA, USA). The RNA for transcriptome were obtained from mixing 20 ± 3-, 300 ± 100-, 1,000 ± 300-, and 1,700 ± 500-year-old individuals of *P. orientalis*, Samples were collected from three trees to provide three replicates. The RNA for gene expression analysis were obtained from 20 ± 3-, 300 ± 100-, 1,000 ± 300-, and 1,700 ± 500-year-old individuals of *P. orientalis* with three biological replicates, respectively.

Construction of a cDNA library and transcriptome sequencing

Oligo (dT) magnetic beads was used to purify mRNA from 20 μg of total RNA. The mRNA was broken into short segments by adding a fragmentation buffer. Short segments with six-base random primers were used as the template for first strand cDNA synthesis. Second strand cDNA synthesis was achieved using dNTPs, RNase H, and DNA polymerase I. Sequencing adapters were ligated onto the short segments after purification according to the protocol of the QiaQuick PCR extraction kit for discriminating different sequencing samples. Segments were selected for PCR amplification and separated by agarose gel electrophoresis as sequencing templates. The Illumina GAIIx system was used to complete sequencing. The sequencing datasets were deposited in the NCBI database (Accession SRX1757589).

Transcriptome assembly and functional annotation

Raw reads were filtered by removing adapter sequences and low-quality reads having a Q20 < 20 bases. Meanwhile, the Q20, Q30, and GC content of the clean data were calculated. High-quality clean sequences were used for further analysis. These clean sequences were *de novo* assembled using Trinity software (*Grabherr et al., 2011*). All of the parameters were set at default values. The parameter of min_kmer_cov was set to 2 as the default, and FPKM values were used to measure each assembled transcript expression level. All of the fragments were mapped onto the non-redundant set of transcripts to quantify the abundance of the assembled transcripts. The longest and optimal assembled sequences were selected as unigenes based on the evaluation and length. Functional annotations were performed by

PeerJ Preprints | https://doi.org/10.7287/peerj.preprints.2866v1 | CC BY 4.0 Open Access | rec: 10 Mar 2017, publ: 10 Mar 2017

homology search against the public databases using unigenes such as Nr and Swiss-Prot using BLASTx with a cutoff E-value of 10-5. Blast2 GO was applied to receive the relevant GO terms based on the Nr BLAST results with E-value<10E-6. Then, unigenes were used for query against the COG and KEGG database to predict and classify functions and pathway assignments (*Tang et al., 2011*).

Quantification of gene expression levels and differential expression analysis

RSEM software was used to estimate the gene expression levels. Clean sequences were mapped back onto the assembled data. Readcounts for each gene were obtained from the mapping results and normalized to FPKM. Before the DGE analysis for each sequenced library, the readcounts were adjusted using the edge R program package by a scaling normalized factor. The DEGseq R package was used for the analysis of the differential expression of two samples. P-values were adjusted using the q-value. q-value < 0.05 and a |log2 (fold change)| > 1 were used to identify significant DEGs. The sequences from the DGE analysis were available at the NCBI database (Accession SRX1755981). To analyze the different age expression patterns of DEGs, K-means clustering was used to cluster the identified DEGs. Complete lists of the DEGs are shown in Supplementary Table S3.

cDNA synthesis by quantitative real-time RT-PCR

Total RNA extraction was performed as described above, and reverse transcriptase reactions were performed using a PrimeScript™ RT reagent Kit (Takara). qRT-PCR (Real-time quantitative PCR) was performed using SYBR® Premix Ex Taq™ II (Tli RNaseH Plus; Takara) in a 20 μL volume containing 10 μL SYBR® primer Ex Taq (2×), 0.8 μL of each primer (10 μM), 2.0 μL of 13-fold diluted cDNA template, and 6.4 μL distilled water. The qRT-PCR program was as follows: 95°C for 10 s, 40 cycles of 95°C for 15 s and annealing at 60°C for 30s. The products were analyzed with a melting curve at the end of the amplification. *αTUB* was selected as the reference gene for *P. orientalis*. Primers were designed with the Primer Premier 3.0 software. Relative gene expression data were quantified using the $2^{-\Delta\Delta CT}$ method with at least three biological replicates. Values of expression levels are means ± standard deviation (SD). Statistical significance was reported at $p < 0.05$.

PeerJ Preprints | https://doi.org/10.7287/peerj.preprints.2866v1 | CC BY 4.0 Open Access | rec: 10 Mar 2017, publ: 10 Mar 2017

RESULTS

Biochemical changes during senescence

During senescence, increased amounts of reactive oxygen species (ROS) are produced along with an increase in proteolytic activity. As shown in Fig. 2, the soluble protein level was high in 20y samples, and then gradually decreasing to a minimum in 1000y samples. The MDA content in the 1700y samples were 1.66 fold ($P < 0.05$) higher than that in the 20y samples. The activities of SOD gradually increased with increasing age, as did the activities of POD, except the activities of POD were minimal in 1700y samples. These results suggested that the extremely ancient *P. orientalis* still retained a good ability to eliminate ROS, although the ancient *P. orientalis* probably had entered the senescence state.

De novo assembly of the *P. orientalis* transcriptome

To characterize the aging events through differentially expressed genes, the three samples of different ages, with three biological replicates for each age were sequenced, and they generated beyond 6.22 Gb, with an average GC content of 45.32% (Supplementary Table S1A), from Illumina HiSeq/MiSeq. The number of clean reads was 62,184,973 (97.2%; Supplementary Fig. S1A). After trimming and assembling, 79,413 transcripts and 48,044 unigenes were generated (Supplementary Fig. S1B; Supplementary Table S1B). Their length distributions are shown in Supplementary Fig. S1C, D. The N50 value of the unigenes was 1,714 bp, with an average length of 896 bp (ranging from 201 to 21,855 bp; Supplementary Table S1B), and 33.96% of the unigenes were longer than 300 bp (Supplementary Fig. S1B). The relative expression level of each unigene was estimated using the FPKM approach and ranged from 0 to 14,810.83 FPKM, with an average of 8.24 FPKM. Of the 48,044 unigenes, 38,202 (79.51%) had very low expression levels of less than 10 FPKM (Supplementary Table S2).

Functional classification of *P. orientalis* unigenes

To verify and annotate the assembled unigenes, all of the assembled sequences were initially

PeerJ Preprints | https://doi.org/10.7287/peerj.preprints.2866v1 | CC BY 4.0 Open Access | rec: 10 Mar 2017, publ: 10 Mar 2017

queried against the NR and SWISS-PROT protein databases, using the BLASTX algorithm. Among the 48,044 unigenes, 24,080 (50.12%) had significant hits in the NR database, and 18,483 (38.47%) had significant matches to proteins in the SWISS-PROT database (Table 1).

Based on the GO catalogues, the annotated unigenes could be categorized into three main classes. As shown in Table 1, 20,029 unigenes were annotated in the GO database. For biological process, the top three abundant unigenes were included in the cellular process (11,580 unigenes), metabolic process (11,322 unigenes), and single-organism process (5,710 unigenes). Only a few unigenes were involved in growth (52 unigenes), cell killing (22 unigenes), and the rhythmic process (8 unigenes). For cellular component, 6,734, 6,717, and 4,910 unigenes belonged to the cell, cell part, and organelle, respectively, while only 1, 1 and 6 unigenes belonged to the synapse, synapse part, and nucleoid, respectively. For molecular function, 11,929 and 10,181 unigenes had binding and catalytic activity, respectively, 1,333 unigenes had transporter activity, and only 4 and 8 unigenes had metallochaperone and receptor regulator activities, respectively (Fig. 3).

In addition, all the unigenes were classified based on the COG database. The COG database classified the putative proteins into at least 25 functional classes (Fig. 4). A total of 1902 unigenes were categorized into general function prediction (R, 1902 unigenes), posttranslational modification (O, 1245 unigenes), signal transduction mechanisms (T, 770 unigenes), and translation (J, 651 unigenes), among which the general function prediction was the largest class.

To further explore the identified unigenes involved in metabolic pathways, we analyzed all unigenes according to the KEGG database. According to the functional annotation, the KEGG pathways could be categorized into five main classes. Among these five classes, the metabolism pathway included the greatest abundance of unigenes. A total of 835 unigenes belonged to carbohydrate metabolism, 610 unigenes belonged to amino acid metabolism, 498 unigenes belonged to energy metabolism, and 482 unigenes belonged to lipid metabolism (Fig. 5).

PeerJ Preprints | https://doi.org/10.7287/peerj.preprints.2866v1 | CC BY 4.0 Open Access | rec: 10 Mar 2017, publ: 10 Mar 2017

Identification of DEGs during senescence

To investigate molecular differences between the four ages, the DEGs between samples were compared. Expression levels were compared between ages to identify significant DEGs by applying a cut off *P*-value < 0.05 (FDR corrected) (Fig. 6A). The most DEGs were in the comparison 1700y/20y (214 DEGs), followed by 1700y/300y (148 DEGs), 300y/20y (81 DEGs), and 1000y/20y (62 DEGs). Noticeably, only 14 DEGs were identified in the 1000y/300y comparison (Fig. 6B). Thus, the gene expression was most divergent between leaves from the youngest (20y) and oldest (1700y) tree in this study, while the gene expression profiles in the leaves from the two middle ages (300y and 1000y) were the most similar, having the least DEGs.

As shown in Fig. 6C, the distribution of DEGs was compared among the three comparisons (300y/20y, 1000y/20y, and 1700y/20y). In total, 17 unigenes were differentially expressed in all three comparisons, while most DEGs (165 of 214) were specifically identified in the comparison 1700y/20y. The results suggested that aging affects gene expression at the transcriptome level. Furthermore, the KEGG pathway enrichment analysis showed that both the photosynthesis (ko00190) and oxidative phosphorylation (ko00195) pathways were significantly enriched in the three comparisons (300y/20y, 1000y/20y, and 1700y/20y), but they were more highly enriched in the 1700y/20y comparison (0.286 for photosynthesis pathway and 0.060 for oxidative phosphorylation pathway) than in the other two comparisons. In addition, metabolic pathways were specifically enriched in the 1700y/20y comparison (Fig. 6D).

Functional classification of the DEGs

To further investigate the functional classification of DEGs, we performed a K-means cluster analysis. In total, eight clusters with distinctive expression patterns were identified (Fig. 7A, Supplementary Table S3). Cluster 4 is the largest subset (136 genes), and its gene expression levels were dramatically decreased in the 1700y samples. The genes in Cluster 3 (32 genes) have expression patterns consistent with those in Cluster 4. The functional classification analysis showed that most of the genes in Clusters 3 and 4 were involved in oxidation reduction, photosynthesis and stress (Fig. 7B). Noticeably, the genes in Cluster 1 (26 genes)

PeerJ Preprints | https://doi.org/10.7287/peerj.preprints.2866v1 | CC BY 4.0 Open Access | rec: 10 Mar 2017, publ: 10 Mar 2017

gradually decreased from 20y to 1700y samples, and their functions were mainly in photosynthesis. The 79 genes classified into Cluster 5 were down-regulated in both 300y and 1000y samples, and their function was mainly in transport. Genes in Cluster 2 (55 genes) gradually increased from 20y to 1700y and mainly functioned in transcription or senescence. The increase in signal transduction and protein process occurred mainly in Clusters 2, 6, 7 and 8. Thus, the genes with different expression patterns were involved in various functions.

Expression profiling of differentially regulated genes by qRT-PCR

To validate RNA-seq data and investigate the dynamic gene expression profiles, we analyzed the expression patterns of eight selected genes by qRT-PCR. The eight genes were *ATP synthase subunit alpha*, *protein suppressor of npr1-1*, *metallothionein-like protein class II*, *probable F-box protein*, *cytochrome oxidase subunit 2* (*COX2*), *NADH dehydrogenase subunit 2*, a putative truncated *TIR-NBS-LRR protein*, and *NADH-ubiquinone oxidoreductase chain 6* (Supplementary Table S4). The expression patterns of the selected genes were consistent between qRT-PCR and RNA-seq data, indicating that our DEG results were reliable (Fig. 8).

Downregulated gene clusters show changes in metabolism and photosynthesis

There are metabolism progress involved in *UDP-glucosyltransferase* (*UGT*) and *Aspartic proteinase nepenthesin-2* (*nep2*) that downregulated with the increasing of *P. orientalis* age (Fig. 9). The expression levels of many photosynthesis-related genes were significantly down-regulated in Cluster 1, together with many others encoding subunits of the *Photosystem (PS) II complexes*. In particular, *Photosystem II reaction center protein Z* (*PSBZ*) and *Photosystem II CP43 chlorophyll apoprotein* (*PSBC*) expression levels in 20y were fourfold lower than those in 1700y samples. In contrast, PSI-related genes were markedly downregulated only from 20y to 1700y samples in Cluster 4, illustrating that PSII was affected more than PSI at *P. orientalis* senescence.

Downregulated gene clusters show changes in transport and oxidation reduction

Transport-related genes such as *Aquaporin PIP2-2*, and *Aquaporin TIP2-1* in Cluster 4, 5 showed significant decreases in expression from 20y to 1700y samples. Genes involved in oxidation reduction, such as *ycf1* (Fig. 9), *cytochrome c oxidase subunit 1* (*COX1*), *COX2*,

PeerJ Preprints | https://doi.org/10.7287/peerj.preprints.2866v1 | CC BY 4.0 Open Access | rec: 10 Mar 2017, publ: 10 Mar 2017

and *ribosomal protein S12* were significantly downregulated in Clusters 1 and 3, with downregulation in ancient *P. orientalis* $1og_2 > 1.5$-fold more than in 20y samples. Cluster 4 is composed of 22 oxidation reduction-related genes that showed significant decreases, $1og_2 > 1$, only from 20y to 1700y samples. Genes involved in photosynthesis and redox reaction expression, such as *cytochrome P450 94A1* (*ATP94A1*) and *dihydroflavonol-4-reductase*, were lower in 1000y samples than in 20y samples.

Upregulated gene clusters show changes in transcription, signal transduction

The expression level of transcription genes involved in *ethylene-responsive transcription factor 1A* (*EREBF*) and *DNAJ* increased with increasing of the *P. orientalis* age in Clusters 2, 7, and 8, indicating that there may be a role for these genes even before senescence (Fig. 9). Signal transduction-related genes involved in *disease resistance protein* (*DRP*) and *Calmodulin-like protein* (*CBP*) in Cluster 2 and 7 were significantly upregulated, with a log2 > 1 value in young *P. orientalis*. Transcription and signal transduction related genes play particularly important roles in protecting ancient *P. orientalis* against senescence under biotic and abiotic stress.

Upregulated gene clusters show changes in protein process and senescence

Protein process-related genes such as *RING-H2 finger protein* and *Aspartic proteinase nepenthesin-2* (*nep2*), and a *senescence-induced receptor-like* (*SIRK*) are increased at *P. orientalis*in with increasing age (Clusters 2 and 7). The up regulation of these genes in the ancient *P. orientalis* compared with the adult tree is consistent with its senescence state.

qRT-PCR analysis validates expression kinetics of photosynthesis related genes and chlorophyll changes during senescence

To validate the reliability of photosynthesis-related gene macroarray analysis results, *Ribulose bisphosphate carboxylase small chain* (*RBCS*) and *YCF2* were selected from the library, and their expression profiles assessed using qRT-PCR. The expression of *RBCS* and *YCF2* decreased in *P. Orientalis* with increasing age (Fig. 10; Supplementary Table S5). These data suggested that photosynthesis in nuclear- and chloroplast-related genes are regulated. Total chlorophyll levels are often used as senescence markers since they are degraded during the

PeerJ Preprints | https://doi.org/10.7287/peerj.preprints.2866v1 | CC BY 4.0 Open Access | rec: 10 Mar 2017, publ: 10 Mar 2017

process. Total chlorophyll, chlorophyll a, and chlorophyll b levels reached a maximum at 20y and then decreased steadily with increasing age, respectively ($P < 0.05$; Fig. 11). The results showed felling trends in chlorophyll levels during senescence. Their expression patterns were mostly consistent with the sequencing results (Fig. 5), which indicated that our DEG results were reliable.

DISCUSSION

There are a limited number of ancient *P. orientalis* in previous studies on senescence (*Buchanan-Wollaston et al., 2005*). Solexa sequencing provides comprehensive and reasonable data resources for plant gene expression analyses (*Tang et al., 2011*; *Deng et al., 2016*). In this study, 20,029 annotated genes were found great differences in *P. orientalis* of different ages, but were mainly concentrated in the 1700y/20y comparison. There were less DEGs in the 1000y/300y comparison, where growth conditions were close. The growth of ancient *P. orientalis* is greatly influenced by their age. The expressions of photosynthesis- and redox-related genes were downregulated substantially, and stress-resistance gene transcription was markedly upregulated with the age-related growth of *P. orientalis*.

Metabolism

There is reduction of metabolism in the ancient *P. orientalis* trees, that consistent with the enzymes involved in *UGT* and *nep2* are known to be induced during senescence in annual plants (*Bajguz and Piotrowska, 2009*). The reasons for grown reduction are complex during the senescence process, so there is a need to study the processes associated with senescence in perennials (*Munné-Bosch and Alegre, 2004*).

Photosynthesis and oxidation-reduction

Photosynthesis degradation is an important step during the senescence process (*Andersson-Gunneråas et al., 2004*; *Hörtensteiner, 2009*). In this study, the total protein and chlorophyll content decreased with increasing age of *P. orientalis*, which was consistent with the process in *Arabidopsis* (*Breeze et al., 2011*). This may be owing to the decline in the

PeerJ Preprints | https://doi.org/10.7287/peerj.preprints.2866v1 | CC BY 4.0 Open Access | rec: 10 Mar 2017, publ: 10 Mar 2017

ability of photosynthesis to change the aging-related transcription of genes including *PSAA*, *PSBZ*, and *ATPF1A* (*Buchanan-Wollaston et al., 2005*; *Ribeiro et al., 2006*; *de Bianchi et al., 2011*). *PSAA* is the reaction center protein of PSI, and the existence of *PSAA/PSAB* polymers is necessary for PSI complex assembly. The light system is an important reactive site for the conversion of light energy into chemical energy (*Amunts et al., 2010*). *PSBZ* is the main site of damage to the photosynthetic apparatus under stress (*Wang et al., 2013*). *ATPF1A* is the key enzyme of energy metabolism (*Zhang et al., 2016*), and its reduction in photosynthesis suggested significant differences between ancient and young trees, as seen with *Pinus ponderosa* (*Breeze et al., 2011*).

The expression levels of these genes involved in *COX1*, *COX2* and *CYP* suggested a significant reduction in the ability to convert chemical energy, which provides energy and respiration for the life activities of ancient *P. orientalis* trees (*Yutaka et al., 2009*). The three largest subunits of the *COX cascade*, *COX1*, *COX2* and *COX3* were downregulated after low temperature stress (*Ott et al., 2007*; *Liu et al., 2015*). Cytochrome P450 is involved in plant secondary metabolism, it is also play an important role in plant resistance to diseases and stresses (*Wang et al., 2016*; *Andersson-Gunnerås et al., 2004*). Mitochondria are the main sites of redox, and genes encoding components of mitochondrial electron transport in *P. orientalis* of different ages needs to be studied further.

Transporter

Transporter related genes involved in *AIG1* were identified that decrease in expression as senescence proceeded in *P. orientalis*. AIG1 proteins are small GTPases originally identified in *Arabidopsis thaliana* where they confer resistance to bacterial infections (*Williams et al., 2011*). Stress genes such as *PRDX* and *HSP90A* were down-regulated in *P. orientalis* trees. *PRDX* reduces hydrogen peroxide, alkylhydroperoxides, and peroxynitrite, and has been detected in a proteomic study of the copper-tolerant species *Scytosiphon gracilis* (*Lovazzano et al., 2013*). *HSP90A* act as molecular chaperones, interacting with other proteins, and can assist in protein folding. The introduction and expression of these genes makes 20y samples resistant to diseases more than in ancient *P. orientalis* trees, but there has been little work on

PeerJ Preprints | https://doi.org/10.7287/peerj.preprints.2866v1 | CC BY 4.0 Open Access | rec: 10 Mar 2017, publ: 10 Mar 2017

395 understanding the regulation of these genes in *P. orientalis*.

396

397 ## Transcription

398 The expression of TFs were upregulated during the senescence process in *Arabidopsis* and
399 *Populus* (*Guo et al., 2004*; *Andersson-Gunneras et al., 2004*; *Zhu et al., 2009*). EREBF and
400 DNAJ were upregulted in ancient *P. orientalis* trees showed that significant consistency
401 between the senescence of 3000y and 20y samples (*Chang et al., 2012*). EREBF responded to
402 low temperature, drought, pathogens and elicitors (*Pandey et al., 2016*; *Gasch et al., 2016*).
403 DNAJ is a member of the *HSP40* family and a molecular chaperone. Alone or in combination
404 with *HSP70*, DNAJ participates in plant growth and development, signal transduction, and
405 resistance to environmental stress (*Shen et al., 2011*). The identification and characterization
406 of transcription factors in *P. orientalis* provides new insights into the molecular mechanisms
407 that regulate transcription factors in the field, and provides information that may be used to
408 improve the stress-tolerance of the trees.

409

410 ## Signal transduction

411 Leaf senescence can be induced by many external cues and internal factors, including heat
412 stress/cold stress, and age. The expression of disease resistance protein and calmodulin-like
413 protein (*CML*) increased with age increasing of ancient *P. orientalis* trees. The diverse roles of
414 *CML* regulated in cell biology: from tissue expression and signaling to disease (*Jeworutzki et*
415 *al., 2010*). *TMV* as a resistance gene avoid infection and protects tobacco against systemic
416 spread of the virus (*Niemeyer et al., 2014*). It is not known how these signals are perceived
417 and subsequently transduced in *P. orientalis*.

418

419 ## Protein synthesis and senescence

420 Senescence may be preceded by an increase in protein synthesis, the majority of cellular
421 proteins such as Aspartic proteinases, are highly expressed in ancient *P. orientalis* trees.
422 Aspartic proteinases participation in processes of apoptosis and programmed cell death (PCD)

PeerJ Preprints | https://doi.org/10.7287/peerj.preprints.2866v1 | CC BY 4.0 Open Access | rec: 10 Mar 2017, publ: 10 Mar 2017

(*Małgorzata et al.*, *2013*). A few *SIRK* have been shown to be upregulated during senescence in *Glycine max*, and *Arabidopsis* (*Martínez et al., 2014*; *Lim et al., 2007*), consistent with their involvement in senescence in ancient *P. orientalis* trees. The study of *P. orientalis* in homologous senescence associated genes functional networks will lead to further understanding of the *P. orientalis* anti-stress effects, and also demonstrate the function of the related genes in the *Arabidopsis* genome database.

CONCLUSIONS

Our analysis of microarray data from 418 different senescence-inducing genes suggests that gene expression profiles from *P. orientalis* of different ages. There were much difference of gene expression mainly in 20y and ancient *P. orientalis* trees, and most of the DEGs showed little difference between 300y and 1000y samples. The results suggested that the middle-aged trees are in similar growing states. Our data shows that metabolism, photosynthesis, oxidation reduction and transporter related genes were clearly reduced in the ancient *P. orientalis* trees, while the upstream regulation of genes such as protein synthesis, transcription, signal transduction and senescence related genes showed that the ancient *P. orientalis* trees might be in a senescent state. Compared to ancient *P. orientalis* trees, the 20y samples contained more of this protective mechanism to resist long-term environment stress. Study on photosynthesis in ancient *P. orientalis* provides new insights at the molecular level that regulate photosynthetic characteristics that may especially enhance the photosynthetic efficiency in trees. This study can provide some theoretical reference for the decline of ancient trees and provide a basis for the protection of ancient *P. orientalis* trees.

ACKNOWLEDGMENTS

Funding

This work was supported by National Non-Profit Research Institutions of Chinese Academy of Forestry [grant numbers: CAFYBB2017ZA007-1, RIF2013-12, RIF2014-11, CAFYBB2014QB004].

Grant Disclosures

PeerJ Preprints | https://doi.org/10.7287/peerj.preprints.2866v1 | CC BY 4.0 Open Access | rec: 10 Mar 2017, publ: 10 Mar 2017

The following grant information was disclosed by the authors:

National Non-Profit Research Institutions of Chinese Academy of Forestry: CAFYBB2017ZA007-1, RIF2013-12, RIF2014-11, and CAFYBB2014QB004. The authors thank the Zhongshan Park (Beijing, China) for providing the *P. orientalis* samples. We also thank Edanz Editing for editing the manuscript.

Competing Interests

The authors declare there are no competing interests.

Author Contributions

Ermei Chang conceived and designed the experiments, performed the experiments, analyzed the data, contributed reagents/materials/analysis tools, wrote the paper, prepared figures and/or tables, reviewed drafts of the paper.

Jin Zhang, Nan Deng, and Xiamei Yao, conceived and designed the experiments, reviewed drafts of the paper.

Zeping Jiang, and Shengqing Shi contributed reagents/materials/analysis tools, reviewed drafts of the paper.

Data Availability

The following information was supplied regarding data availability: The National Center for Biotechnology Information (NCBI) Sequence Read Archive (SRA) database (accession number: SRX1757589 and SRX1755981).

PeerJ Preprints | https://doi.org/10.7287/peerj.preprints.2866v1 | CC BY 4.0 Open Access | rec: 10 Mar 2017, publ: 10 Mar 2017

REFERENCES

Amunts A, Toporik H, Borovikova A, Nelson N. 2010. Structure determination and improved model of plant photosystem I. *Journal of Biological Chemistry* **285 (5):**3478-3486. DOI 10.1074/jbc.M109.072645.

Andersson A, Keskitalo J, Sjödin A, Bhalerao R, Sterky F, Wissel K, Tandre K, Aspeborg H, Moyle R, Ohmiya Y. 2004. A transcriptional timetable of autumn senescence. *Genome Biology* **5 (4):**1-13. DOI 10.1186/gb-2004-5-4-r24.

Andersson Gunnerås S, Mellerowicz EJ, Love J, Segerman B, Ohmiya Y, Coutinho PM, Nilsson P, Henrissat B, Moritz T, Sundberg B. 2006. Biosynthesis of cellulose‐enriched tension wood in Populus: global analysis of transcripts and metabolites identifies biochemical and developmental regulators in secondary wall biosynthesis. *The Plant Journal* **45(2):**144-165. DOI 10.1111/j.1365-313X.2005.02584.x.

Bajguz A, and Piotrowska A. 2009. Conjugates of auxin and cytokinin. *Phytochemistry* **70**: 957. DOI 0.1016/j.phytochem.2009.05.006.

Bhalerao R, Keskitalo J, Sterky F, Erlandsson R, Björkbacka H, Birve SJ, Karlsson J, Gardeström P, Gustafsson P, Lundeberg J. 2003. Gene expression in autumn leaves. *Plant Physiology* **131 (2):**430-442. DOI org/ 10. 1104/ pp. 012732.

Bond BJ. 2000. Age-related changes in photosynthesis of woody plants. *Trends in plant science* **5 (8):**349-353. DOI 10.1016/S1360-1385(00)01691-5.

Breeze E, Harrison E, McHattie S, Hughes L, Hickman R, Hill C, Kiddle S, Kim Y, Penfold CA, Jenkins D. 2011. High-resolution temporal profiling of transcripts during *Arabidopsis* leaf senescence reveals a distinct chronology of processes and regulation. *The Plant Cell* **23 (3):**873-894. DOI org/ 10. 1105/ tpc. 111. 083345.

Buchanan Wollaston V, Page T, Harrison E, Breeze E, Lim PO, Nam HG, Lin JF, Wu SH, Swidzinski J, Ishizaki K. 2005. Comparative transcriptome analysis reveals significant differences in gene expression and signalling pathways between developmental and dark/starvation‐induced senescence in *Arabidopsis*. *The Plant Journal* **42 (4):**567-585. DOI 10.1111/j.1365-313X.2005.02399.x.

Chang E, Shi S, Liu J, Cheng T, Xue L, Yang X, Yang W, Lan Q, Jiang Z. 2012. Selection of reference genes for quantitative gene expression studies in *Platycladus orientalis* (Cupressaceae) using real-time PCR. *PloS one* **7 (3):**e33278. DOI org/10.1371/journal.pone.0033278.

Chang E, Zhao Y, Wei Q, Shi S, Jiang Z. 2016. Isolation of high-quality RNA from *Platycladus orientalis* and

PeerJ Preprints | https://doi.org/10.7287/peerj.preprints.2866v1 | CC BY 4.0 Open Access | rec: 10 Mar 2017, publ: 10 Mar 2017

other Cupressaceae plants. *Electronic Journal of Biotechnology* **23:** 21-27. DOI org/10.1016/j.ejbt.2016.08.003.

Cui Z, Bi W, Hao X, Xu Y, Li P, Walker MA, Wang Q. 2016. Responses of in vitro-grown plantlets (*Vitis vinifera*) to grapevine leafroll-associated virus-3 and PEG-induced drought stress. *Frontiers in Physiology* **7:**203. DOI 10.3389/fphys.2016.00203.

de Bianchi S, Betterle N, Kouril R, Cazzaniga S, Boekema E, Bassi R, Dall Osto L. 2011. *Arabidopsis* mutants deleted in the light-harvesting protein *Lhcb4* have a disrupted photosystem II macrostructure and are defective in photoprotection. *The Plant Cell* **23 (7):**2659-2679. DOI org/ 10. 1105/ tpc. 111. 087320.

Deng N, Chang E, Li M, Ji J, Yao X, Bartish IV, Liu J, Ma J, Chen L, Jiang Z. 2016. Transcriptome characterization of gnetum parvifolium reveals candidate genes involved in important secondary metabolic pathways of flavonoids and stilbenoids. *Frontiers in Plant Science* **7 (222)**. DOI 10.3389/fpls.2016.00174.

Dhindsa RS, Plumb-Dhindsa P, Thorpe TA. 1981. Leaf senescence: correlated with increased levels of membrane permeability and lipid peroxidation, and decreased levels of superoxide dismutase and catalase. *Journal of Experimental Botany* **32 (1):**93-101.

Duan D, Fischer S, Merz P, Bogs J, Riemann M, Nick P. 2016. An ancestral allele of grapevine transcription factor MYB14 promotes plant defence. *Journal of experimental botany* v569. DOI 10.1093/jxb/erv569.

Flanary BE, Kletetschka G. 2005. Analysis of telomere length and telomerase activity in tree species of various life-spans, and with age in the bristlecone pine *Pinus longaeva*. *Biogerontology* **6 (2):**101-111. DOI 10.1007/s10522-005-3484-4.

Franco AC, Soyza AGD, Virginia RA, Reynolds JF, Whitford WG. 1994. Effects of plant size and water relations on gas exchange and growth of the desert shrub *Larrea tridentata*. *Oecologia* **97 (2):**171-178. DOI 10.1007/BF00323146.

Gasch P, Fundinger M, Müller JT, Lee T, Bailey-Serres J, Mustroph A. 2015. Redundant ERF-VII transcription factors bind an evolutionarily-conserved cis-motif to regulate hypoxia-responsive gene expression in *Arabidopsis*. *The Plant Cell* C2015-C2866. DOI org/ 10. 1105/ tpc. 15. 00866.

Gonzales DH, Neupert W. 1990. Biogenesis of mitochondrialc-type cytochromes. *Journal of bioenergetics and biomembranes* **22 (6):**753-768. DOI 10.1007/BF00786929.

Guo Y, Cai Z, Gan S. 2004. Transcriptome of *Arabidopsis* leaf senescence. *Plant, cell & environment* **27 (5):**521-549. DOI 10.1111/j.1365-3040.2003.01158.x.

PeerJ Preprints | https://doi.org/10.7287/peerj.preprints.2866v1 | CC BY 4.0 Open Access | rec: 10 Mar 2017, publ: 10 Mar 2017

Gupta DK, Pena LB, Romero Puertas MC, Hernández A, Inouhe M, Sandalio LM. 2016. NADPH oxidases differentially regulate ROS metabolism and nutrient uptake under cadmium toxicity. *Plant Cell & Environment*. DOI 10.1111/pce.12711.

Hayashi K, Fujita Y, Ashizawa T, Suzuki F, Nagamura Y, Hayano Saito Y. 2016. Serotonin attenuates biotic stress and leads to lesion browning caused by a hypersensitive response to *Magnaporthe oryzae* penetration in rice. *The Plant Journal* **85 (1):**46-56. DOI 10.1111/tpj.13083.

Heath RL, Packer L. 1968. Photoperoxidation in isolated chloroplasts : I. Kinetics and stoichiometry of fatty acid peroxidation. *Archives of Biochemistry & Biophysics* **125 (1):**189-198. DOI .org/10.1016/0003-9861(68)90654-1.

Hörtensteiner S. 2009. Stay-green regulates chlorophyll and chlorophyll-binding protein degradation during senescence. *Trends in plant science* **14 (3):**155-162. DOI 10.1016/j.tplants.2009.01.002.

Huang J, Gu M, Lai Z, Fan B, Shi K, Zhou YH, Yu JQ, Chen Z. 2010. Functional analysis of the *Arabidopsis PAL* gene family in plant growth, development, and response to environmental stress. *Plant Physiology* **153 (153):**1526-1538. DOI org/ 10. 1104/ pp. 110. 157370.

Issartel J, Coiffard C. 2011. Extreme longevity in trees: live slow, die old? *Oecologia* 165 (1):1-5. DOI 10.1007/s00442-010-1807-x.

Jeworutzki E, Roelfsema MR, Anschütz U, Krol E, Elzenga JT, Felix G, Boller T, Hedrich R, and Becker D. 2010. Early signaling through the *Arabidopsis* pattern recognition receptors FLS2 and EFR involves Ca-associated opening of plasma membrane anion channels. *Plant Journal* **62**: 367 – 378. DOI 10.1111/j.1365-313X.2010.04155.x.

Keskitalo J, Bergquist G, Gardeström P, Jansson S. 2005. A cellular timetable of autumn senescence. *Plant Physiology* **139 (4):**1635-1648. DOI org/ 10. 1104/ pp. 105.

Klimešová J, Nobis MP, Herben T. 2015. Senescence, ageing and death of the whole plant: morphological prerequisites and constraints of plant immortality. *New Phytologist* **206 (1):**14-18. DOI 10.1111/nph.13160.

Lanner RM, Connor KF. 2001. Does bristlecone pine senesce? *Experimental gerontology* **36 (4):**675-685. DOI 10.1016/S0531-5565(00)00234-5.

Lim PO, Hong GN, Lim PO, Hong GN. 2005. The molecular and genetic control of leaf senescence and longevity in *Arabidopsis*. *Current Topics in Developmental Biology* **67:**49-83. DOI 10.1016/S0070-2153(05)67002-0.

Lim PO, Kim HJ, Gil Nam H. 2007. Leaf senescence. *Annu. Rev. Plant Biol.* 58:115-136. DOI

PeerJ Preprints | https://doi.org/10.7287/peerj.preprints.2866v1 | CC BY 4.0 Open Access | rec: 10 Mar 2017, publ: 10 Mar 2017

10.1146/annurev.arplant.57.032905.105316.

Liu A, Chen S, Wang M, Wang Z, Zheng C, Zhao P, Guo D, Ahammed GJ. 2015. Silencing of mitochondrial uncoupling protein gene aggravates chilling stress by altering mitochondrial respiration and electron transport in tomato. *Acta Physiologiae Plantarum* 37 (11):1-9. DOI 10.1007/s11738-015-1974-9.

Małgorzata G, Piotr L, and Krystyna R. 2013. Two-dimensional zymography in detection of proteolytic enzymes in wheat leaves. *Acta Physiologiae Plantarum* **35**: 3477-3482. DOI 10.1007/s11738-013-1371-1.

Martínez DE, and Guiamet JJ. 2014. Senescence-Related Changes in the Leaf Apoplast. *Journal of Plant Growth Regulation* **33**: 44-55. DOI 10.1007/s00344-013-9395-8.

Munné-Bosch S. 2007. Aging in perennials. *Critical Reviews in Plant Sciences* **26 (3):**123-138. DOI 10.1080/07352680701402487.

Munné-Bosch S. 2008. Do perennials really senesce? *Trends in plant science* **13 (5):**216-220. DOI 10.1016/j.tplants.2008.02.002.

Munnebosch S, Alegre L. 2004. Review: Die and let live: leaf senescence contributes to plant survival under drought stress. *Functional Plant Biology* **31 (3):**8808-8818. DOI 10.1071/FP03236.

Munné-Bosch S, Alegre L. 2002. Plant aging increases oxidative stress in chloroplasts. *Planta* **214 (4):**608-615. DOI 10.1007/s004250100646.

Nemoto S, Finkel T. 2004. Ageing and the mystery at Arles. *Nature* **429 (6988):**149-152. DOI 10.1038/429149a.

Niemeyer J, Ruhe J, Machens F, Stahl DJ, and Hehl R. 2014. Inducible expression of p50 from TMV for increased resistance to bacterial crown gall disease in tobacco. *Plant Molecular Biology* **84**: 111-123. DOI 10.1007/s11103-013-0122-4.

Ott M, Gogvadze V, Orrenius S, Zhivotovsky B. 2007. Mitochondria, oxidative stress and cell death. *Apoptosis* **12 (5):**913-922. DOI 10.1007/s10495-007-0756-2.

Palma JM, Río LAD. 2006. Antioxidative enzymes from chloroplasts, mitochondria, and peroxisomes during leaf senescence of nodulated pea plants. *Journal of Experimental Botany* **57 (8):**1747-1758. DOI org/10.1093/jxb/erj191.

Pandey B, Sharma P, Tyagi C, Goyal S, Grover A, Sharma I. 2016. Structural modeling and molecular simulation analysis of HvAP2/EREBP from barley. *Journal of Biomolecular Structure and Dynamics* **34 (6):**1159-1175. DOI org/10.1080/07391102.2015.1073630.

Peñuelas J. 2005. Plant physiology: a big issue for trees. *Nature* 437 (7061):965-966. DOI 10.1038/437965a.

Reich PB, Tjoelker MG, Machado J, Oleksyn J. 2006. Universal scaling of respiratory metabolism, size and nitrogen in plants. *Nature* **439 (7075)**:457-461. DOI 10.1038/nature04282.

Ribeiro AC, Ascunce GI, Rocha-Lima CS, Levi JU, Sleeman D, Dorsett D, Merchan J. 2006. The role of sugars in integrating environmental signals during the regulation of leaf senescence. *Journal of Experimental Botany* **57 (2):**391-399. DOI 10.1093/jxb/eri279.

Shen L, Kang YGG, Liu L, Yu H. 2011. The J-domain protein J3 mediates the integration of flowering signals in *Arabidopsis*. *The Plant Cell* **23 (2):**499-514. DOI org/ 10. 1105/ tpc. 111. 083048.

Sillett SC, Van Pelt R, Carroll AL, Kramer RD, Ambrose AR, Trask D. 2015. How do tree structure and old age affect growth potential of California redwoods? *Ecological Monographs* **85 (2):**181-212. DOI 10.1890/14-1016.1.

Sun HK, Sang HK, Palaniyandi SA, Yang SH, Suh JW. 2015. Expression of potato S -adenosyl- l -methionine synthase (*SbSAMS*) gene altered developmental characteristics and stress responses in transgenic *Arabidopsis* plants. *Plant Physiology & Biochemistry* **87:**84-91. DOI 10.1016/j.plaphy.2014.12.020.

Sun X, Sun C, Li Z, Hu Q, Han L, Luo H. 2016. *AsHSP17*, a creeping bentgrass small heat shock protein modulates plant photosynthesis and ABA - dependent and independent signalling to attenuate plant response to abiotic stress. *Plant, cell & environment*. DOI 10.1111/pce.12683.

Tang Q, Ma X, Mo C, Wilson IW, Song C, Zhao H, Yang Y, Fu W, Qiu D. 2011. An efficient approach to finding *Siraitia grosvenorii* triterpene biosynthetic genes by RNA-seq and digital gene expression analysis. *Ecological Monographs* **12 (1):**1. DOI 10.1186/1471-2164-12-343.

Thomas H. 2013. Senescence, ageing and death of the whole plant. *New Phytologist* 197 (3):696-711. DOI 10.1111/nph.12047.

Tillmann B, Röth S, Bublak D, Sommer M, Stelzer EHK, Scharf KD, Schleiff E. 2014. Hsp90 is involved in the regulation of cytosolic precursor protein abundance in tomato. *Molecular Plant* **8 (2):**228-241. DOI 10.1016/j.molp.2014.10.005.

Wagstaff C, Yang TJ, Stead AD, Buchanan Wollaston V, Roberts JA. 2009. A molecular and structural characterization of senescing *Arabidopsis* siliques and comparison of transcriptional profiles with senescing petals and leaves. *The Plant Journal* **57 (4):**690-705. DOI 10.1111/j.1365-313X.2008.03722.x.

Wang C, Yang Y, Wang H, Ran X, Li B, Zhang J, Zhang H. 2016. Ectopic expression of a cytochrome P450 monooxygenase gene *PtCYP714A3* from *Populus trichocarpa* reduces shoot growth and improves tolerance to salt stress in transgenic rice. *Plant biotechnology journal*. DOI 10.1111/pbi.12544.

PeerJ Preprints | https://doi.org/10.7287/peerj.preprints.2866v1 | CC BY 4.0 Open Access | rec: 10 Mar 2017, publ: 10 Mar 2017

Wang P, Sun X, Li C, Wei Z, Liang D, Ma F. 2013. Long–term exogenous application of melatonin delays drought - induced leaf senescence in apple. *Journal of Pineal Research* **54 (3):**292-302. DOI 10.1111/jpi.12017.

Watson J, Riha K. 2010. Telomeres, aging, and plants: from weeds to Methuselah – a mini-review. *Gerontology* **57 (2):**129-136. DOI 10.1159/000310174.

Williams SJ, Sornaraj P, Decourcy-Ireland E, Menz RI, Kobe B, Ellis JG, Dodds PN, and Anderson PA. 2011. An autoactive mutant of the M flax rust resistance protein has a preference for binding ATP, whereas wild-type M protein binds ADP. *Mol Plant Microbe Interact.* **24**: 897-906. DOI org/10.1094/MPMI-03-11-0052.

Yutaka S, Morita R, Katsuma S, Nishimura M, Tanaka A, Kusaba M. 2008. Two short-chain dehydrogenase/reductases, *NON-YELLOW COLORING 1* and *NYC1-LIKE*, are required for chlorophyll b and light-harvesting complexII degradation during senescence in rice. *Plant Journal* **57 (1):**120-131. DOI 10.1111/j.1365-313X.2008.03670.x.

Zhang C, Liu J, Zhao T, Gomez A, Li C, Yu C, Li H, Lin J, Yang Y, Liu B. 2016. A Drought-inducible bZIP Transcription Factor OsABF1 Delays Reproductive Timing in Rice. PLANT PHYSIOL **171 (1)**. DOI 10.1104/pp.16.01691.

Zhang F, Xu T, Mao L, Yan S, Chen X, Wu Z, Chen R, Luo X, Xie J, Gao S. 2016. Genome-wide analysis of Dongxiang wild rice (*Oryza rufipogon* Griff.) to investigate lost/acquired genes during rice domestication. *BMC plant biology* 16 (1):1. DOI 10.1007/s11103-009-9538-2.

Zhu Y, Wang Z, Jing Y, Wang L, Liu X, Liu Y, Deng X. 2009. Ectopic over-expression of , a heat shock factor from the resurrection plant , leads to increased thermotolerance and retarded growth in transgenic and tobacco. *Plant Molecular Biology* DOI 10.1007/s11103-009-9538-2.

Figure Captions

Fig. 1. The trees sampled were 20, 1300, 1,000, and 1,700 years old (y) individuals of *Platycladus orientalis* in Zhongshan Park, Beijing.

PeerJ Preprints | https://doi.org/10.7287/peerj.preprints.2866v1 | CC BY 4.0 Open Access | rec: 10 Mar 2017, publ: 10 Mar 2017

Fig. 2. SOD and POD activity, the content of MDA and total protein. Components of stilbenes. Vertical bars represent the mean ± SD of four separate experiments. Data were analyzed by ANOVA in the SPASS software.

Fig. 3. Gene Ontology (GO) classifications of assembled unigenes.

Main functional categories in biological process, cellular component, and molecular functions relevant to plant physiology. Bars represent the number of *Platycladus orientalis* assigned proteins with BLASTX matches to each GO term. One unigene may be matched to multiple GO terms.

Fig. 4. Clusters of orthologous groups (COG) classification.

In total, 4,044 unigenes with Nr hits were grouped into 26 KOG terms. The *y*-axis represents the percentage of all unigenes.

Fig. 5. Functional annotation of unigenes based on KEGG categorization.

Main functional categories are summarized as follows: **(A)** Cellular processes, **(B)** Environmental information processing, **(C)** Genetic information processing, **(D)** Metabolism, and **(E)** Organismal systems. Bars represent the number of *Platycladus orientalis* assigned unigenes with BLASTX matches to each KEGG term. The *x*-axis indicates the number of genes annotated under the pathway out of the total number of genes annotated (%).

Fig. 6. Analysis of DEGs among the four *Platycladus orientalis* ages.

(A) Number of DEGs in pairwise comparisons; **(B)** A Venn diagram of the numbers of unique and common DEGs between different stages; **(C)** Significantly enriched KEGG pathway terms (corrected *P*-value < 0.05) in three comparisons (300y/20y, 1000y/20y, and 1700y/20y).

Fig. 7. K-Means clustering of gene expression profiles.

(A) The centers of eight clusters with different expression patters. The number of genes in each cluster is labeled; **(B)** Functional classification of each cluster.

PeerJ Preprints | https://doi.org/10.7287/peerj.preprints.2866v1 | CC BY 4.0 Open Access | rec: 10 Mar 2017, publ: 10 Mar 2017

Fig. 8. Expression patterns of eight selected unigenes in *Platycladus orientalis* leaves using qRT-PCR.

Verification of eight selected DEGs by qRT-PCR. Red lines indicate the results from qRT-PCR, and blue lines indicate the results from RNA-seq. *αTUB* was used as the internal control. Both methods show similar gene expression trends. Three biological replicates were performed.

Fig. 9. Differential gene expression significantly over-represented by positive or negative gene expression gradients that highlight different ages of *Platycladus orientalis*.

Fig. 10. Expression patterns of photosynthesis-related unigenes in *Platycladus orientalis* leaves.

Verification of eight selected DEGs by qRT-PCR. The red column contains the results from qRT-PCR and the blue column contains the results from RNA-seq. *αTUB* was used as the internal control. Both methods show similar gene expression trends. Three biological replicates were performed.

Fig. 11. Chlorophyll a, chlorophyll b, and total chlorophyll content.

Vertical bars represent the mean ± SD of four separate experiments. Data were analyzed by ANOVA in the SPASS software.

Table Captions

Table 1. Functional annotation of the *Platycladus orientalis* transcriptome.

Supplementary Material

Supplementary Fig. S1 | Overview of *Platycladus orientalis* tanscriptome sequencing and assembly. (A) Classification of raw reads after filtering and trimming adapters; (B) Transcript and Unigene length interval, the x-axis represents the length interval; (C/D) Transcript/unigene length distribution, the y-axis represents the length frequency.

PeerJ Preprints | https://doi.org/10.7287/peerj.preprints.2866v1 | CC BY 4.0 Open Access | rec: 10 Mar 2017, publ: 10 Mar 2017

713 **Supplementary table S1** | Summaries of transcriptome sequencing and assembly for
714 *Platycladus orientalis*.

715 **Supplementary table S2** | Read counts and FPKM values of *Platycladus orientalis* unigenes.

716 **Supplementary table S3** K-Means clustering of gene expression profiles.

717 **Supplementary table S4** Primers of candidate genes for qRT-PCR in Fig. 8.

718 **Supplementary table S5** Primers of photosynthesis related unigenes for qRT-PCR in Fig. 10.

719 **Supplementary File** Zhongshan Park (Beijing, China) for providing the *P. orientalis* samples.

720

721

PeerJ Preprints | https://doi.org/10.7287/peerj.preprints.2866v1 | CC BY 4.0 Open Access | rec: 10 Mar 2017, publ: 10 Mar 2017

722 **Fig. 1. The trees sampled were 20, 1300, 1,000, and 1,700 years old (y) individuals of**
723 ***Platycladus orientalis* in Zhongshan Park, Beijing.**

724

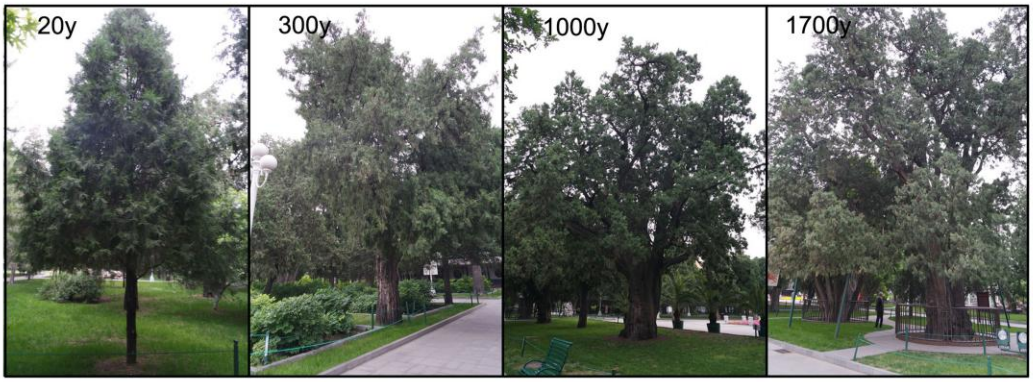

725
726
727
728
729
730
731
732
733
734
735
736
737

PeerJ Preprints | https://doi.org/10.7287/peerj.preprints.2866v1 | CC BY 4.0 Open Access | rec: 10 Mar 2017, publ: 10 Mar 2017

738 **Fig. 2. SOD and POD activity, the content of MDA and total protein.** Components of
739 stilbenes. Vertical bars represent the mean ± SD of four separate experiments. Data were
740 analyzed by ANOVA in the SPASS software.

741

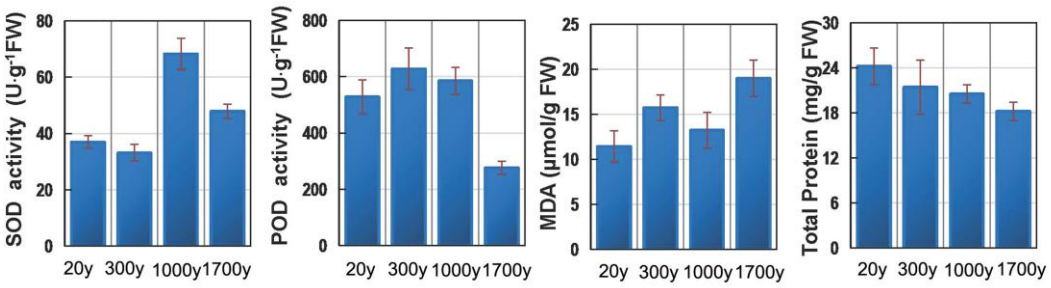

742

743

744

745

PeerJ Preprints | https://doi.org/10.7287/peerj.preprints.2866v1 | CC BY 4.0 Open Access | rec: 10 Mar 2017, publ: 10 Mar 2017

Fig. 3. Gene Ontology (GO) classifications of assembled unigenes.

Main functional categories in biological process, cellular component, and molecular functions relevant to plant physiology. Bars represent the number of *Platycladus orientalis* assigned proteins with BLASTX matches to each GO term. One unigene may be matched to multiple GO terms.

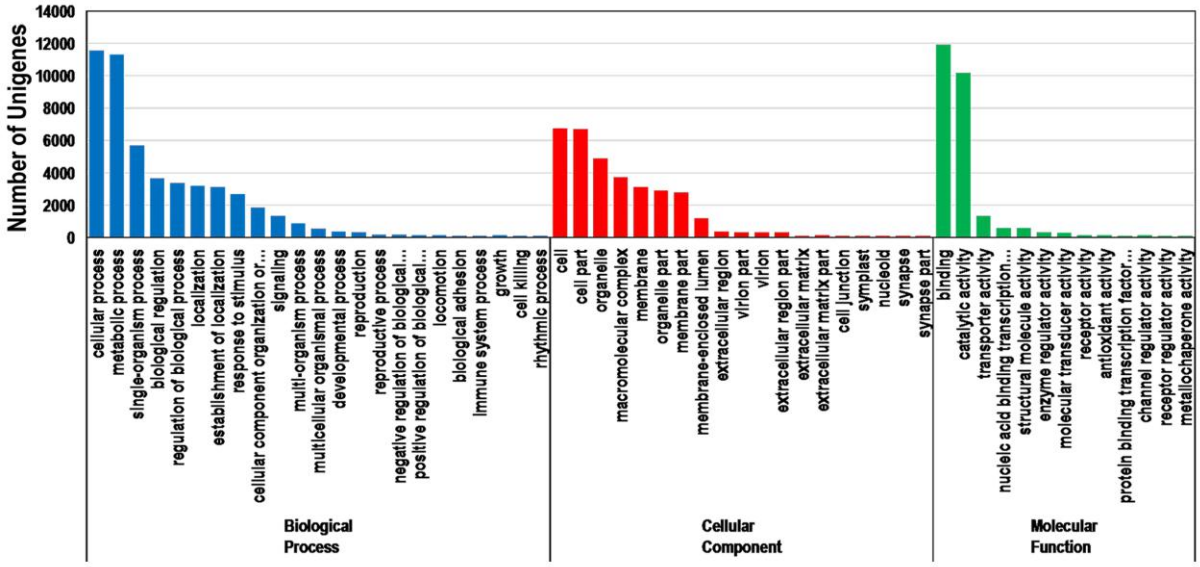

PeerJ Preprints | https://doi.org/10.7287/peerj.preprints.2866v1 | CC BY 4.0 Open Access | rec: 10 Mar 2017, publ: 10 Mar 2017

Fig. 4. Clusters of orthologous groups (COG) classification.

In total, 4,044 unigenes with Nr hits were grouped into 26 KOG terms. The *y*-axis represents the percentage of all unigenes.

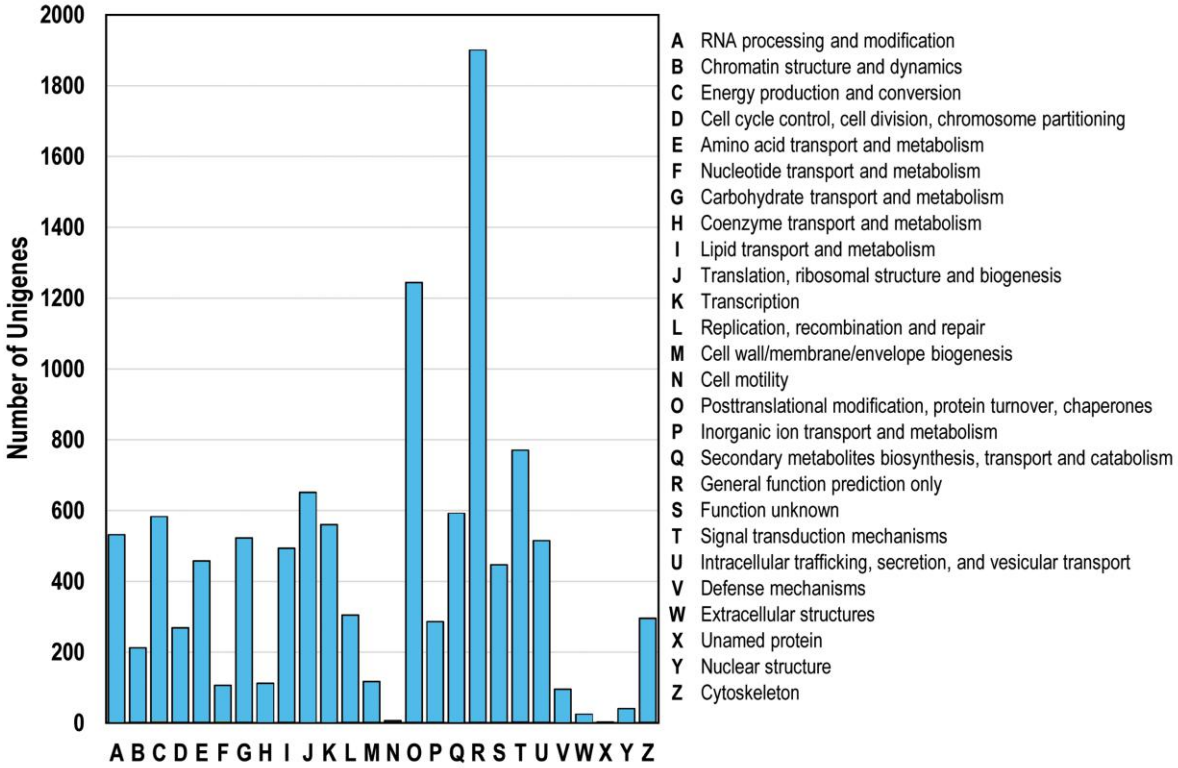

PeerJ Preprints | https://doi.org/10.7287/peerj.preprints.2866v1 | CC BY 4.0 Open Access | rec: 10 Mar 2017, publ: 10 Mar 2017

764 **Fig. 5. Functional annotation of unigenes based on KEGG categorization.**

765 Main functional categories are summarized as follows: **(A)** Cellular processes, **(B)**
766 Environmental information processing, **(C)** Genetic information processing, **(D)** Metabolism,
767 and **(E)** Organismal systems. Bars represent the number of *Platycladus orientalis* assigned
768 unigenes with BLASTX matches to each KEGG term. The *x*-axis indicates the number of
769 genes annotated under the pathway out of the total number of genes annotated (%).

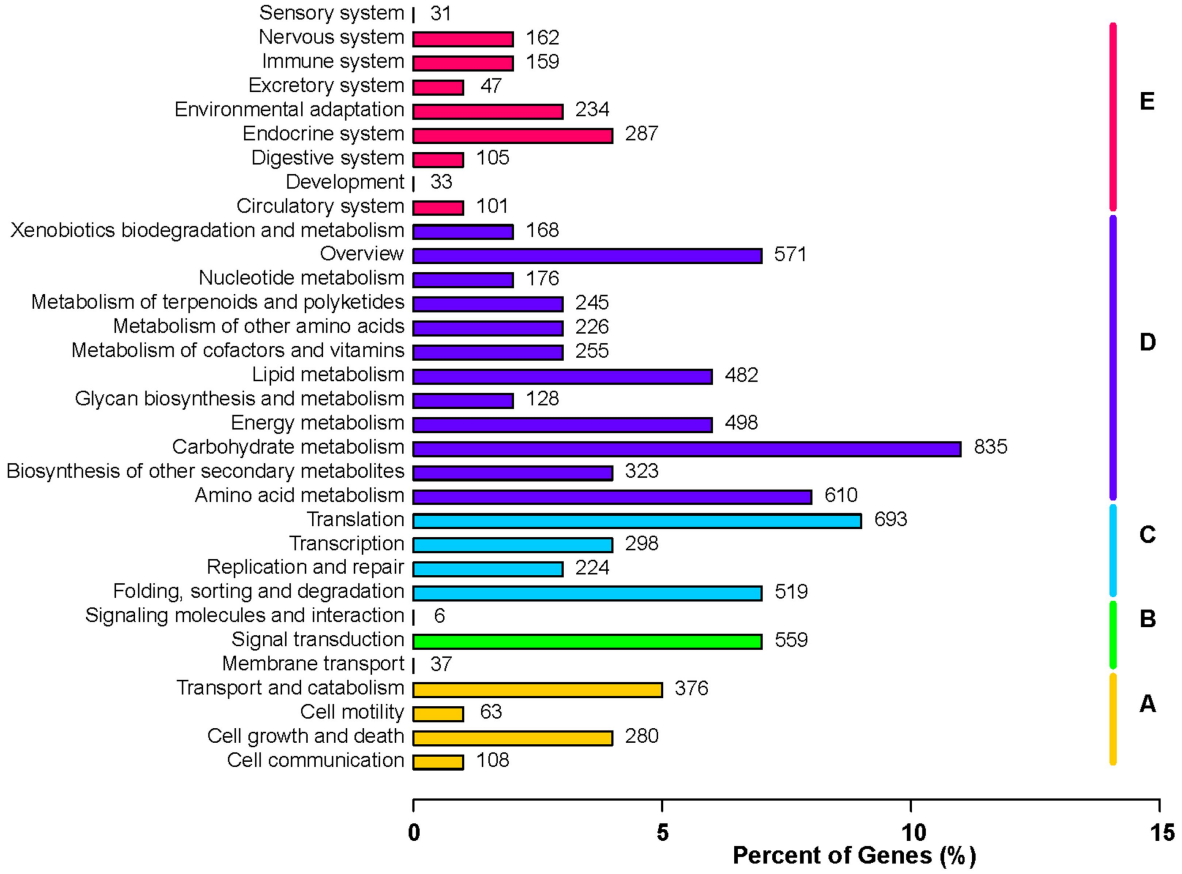

770
771
772
773

PeerJ Preprints | https://doi.org/10.7287/peerj.preprints.2866v1 | CC BY 4.0 Open Access | rec: 10 Mar 2017, publ: 10 Mar 2017

Fig. 6. Analysis of DEGs among the four *Platycladus orientalis* ages.

(B) Number of DEGs in pairwise comparisons; **(B)** A Venn diagram of the numbers of unique and common DEGs between different stages; **(C)** Significantly enriched KEGG pathway terms (corrected *P*-value < 0.05) in three comparisons (300y/20y, 1000y/20y, and 1700y/20y).

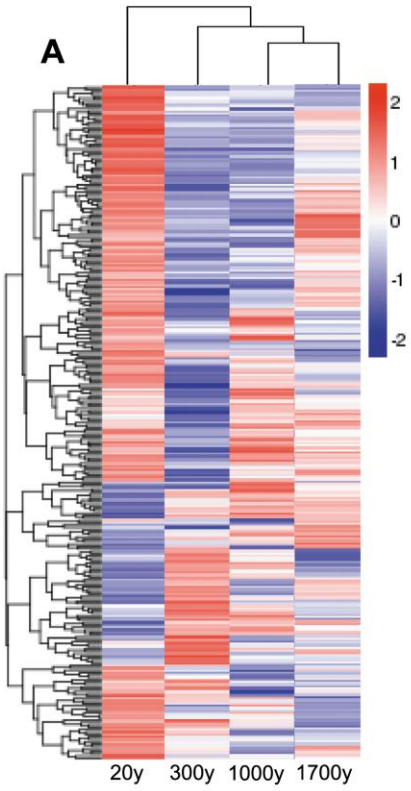

B

	DEGs	Up-regulated	Down-regulated
300y / 20y	81	24	57
1000y / 20y	62	12	50
1700y / 20y	214	48	166
1000y / 300y	14	5	9
1700y / 300y	148	56	92
1700y / 1000y	56	31	25

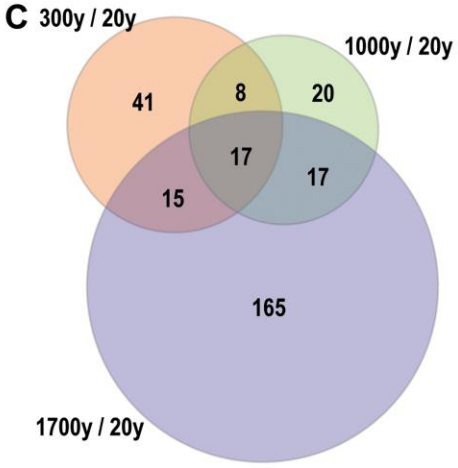

D

KEGG Term	Pathway ID	Sample number	Background number	Rich factor	Corrected *P*-Value
300y / 20y					
Photosynthesis	ko00190	3	42	0.071	0.032
Oxidative phosphorylation	ko00195	5	183	0.027	0.032
1000y / 20y					
Photosynthesis	ko00195	4	42	0.095	0.000
Oxidative phosphorylation	ko00190	5	183	0.027	0.002
1700y / 20y					
Photosynthesis	ko00195	12	42	0.286	0.000
Oxidative phosphorylation	ko00190	11	183	0.060	0.000
Metabolic pathways	ko01100	28	2007	0.014	0.016

PeerJ Preprints | https://doi.org/10.7287/peerj.preprints.2866v1 | CC BY 4.0 Open Access | rec: 10 Mar 2017, publ: 10 Mar 2017

783

784 **Fig. 7. K-Means clustering of gene expression profiles.**

785 **(B)** The centers of eight clusters with different expression patters. The number of genes in

786 each cluster is labeled; **(B)** Functional classification of each cluster.

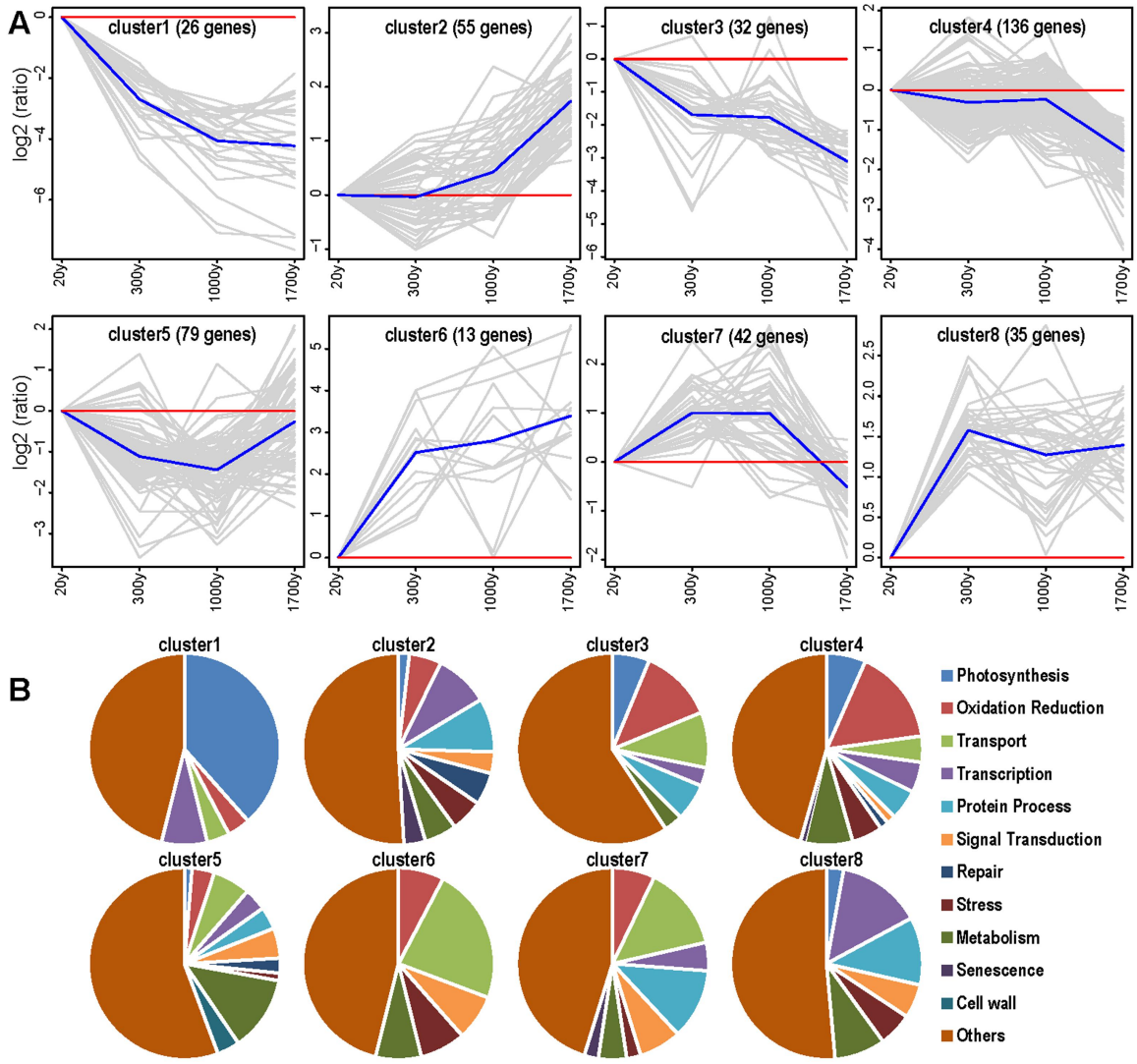

787

788

789

PeerJ Preprints | https://doi.org/10.7287/peerj.preprints.2866v1 | CC BY 4.0 Open Access | rec: 10 Mar 2017, publ: 10 Mar 2017

Fig. 8. Expression patterns of eight selected unigenes in *Platycladus orientalis* leaves using qRT-PCR.

Verification of eight selected DEGs by qRT-PCR. Red lines indicate the results from qRT-PCR, and blue lines indicate the results from RNA-seq. *αTUB* was used as the internal control. Both methods show similar gene expression trends. Three biological replicates were performed.

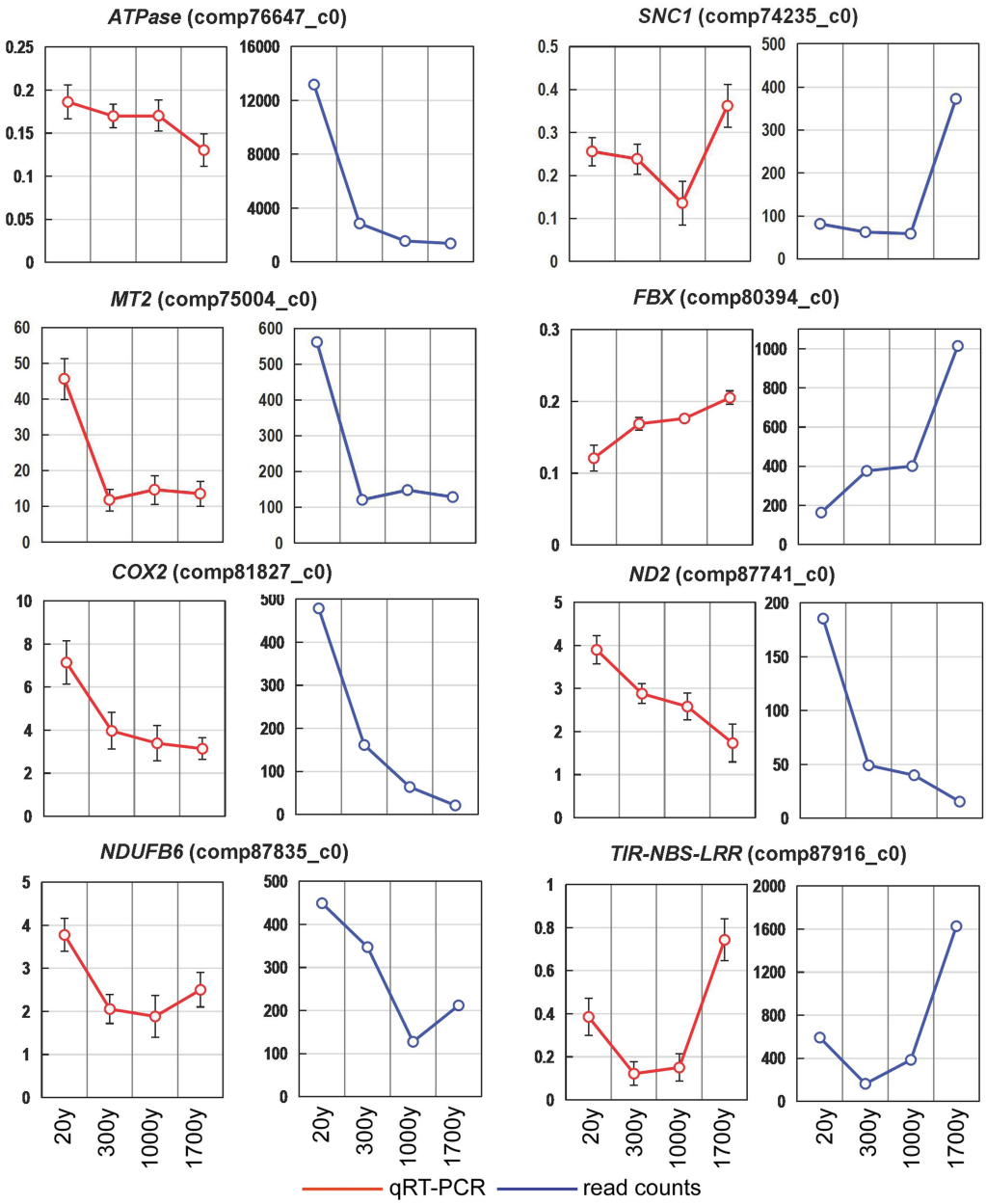

PeerJ Preprints | https://doi.org/10.7287/peerj.preprints.2866v1 | CC BY 4.0 Open Access | rec: 10 Mar 2017, publ: 10 Mar 2017

800

801 **Fig. 9. Differential gene expression significantly over-represented by positive or negative**

802 **gene expression gradients that highlight different ages of *Platycladus orientalis*.**

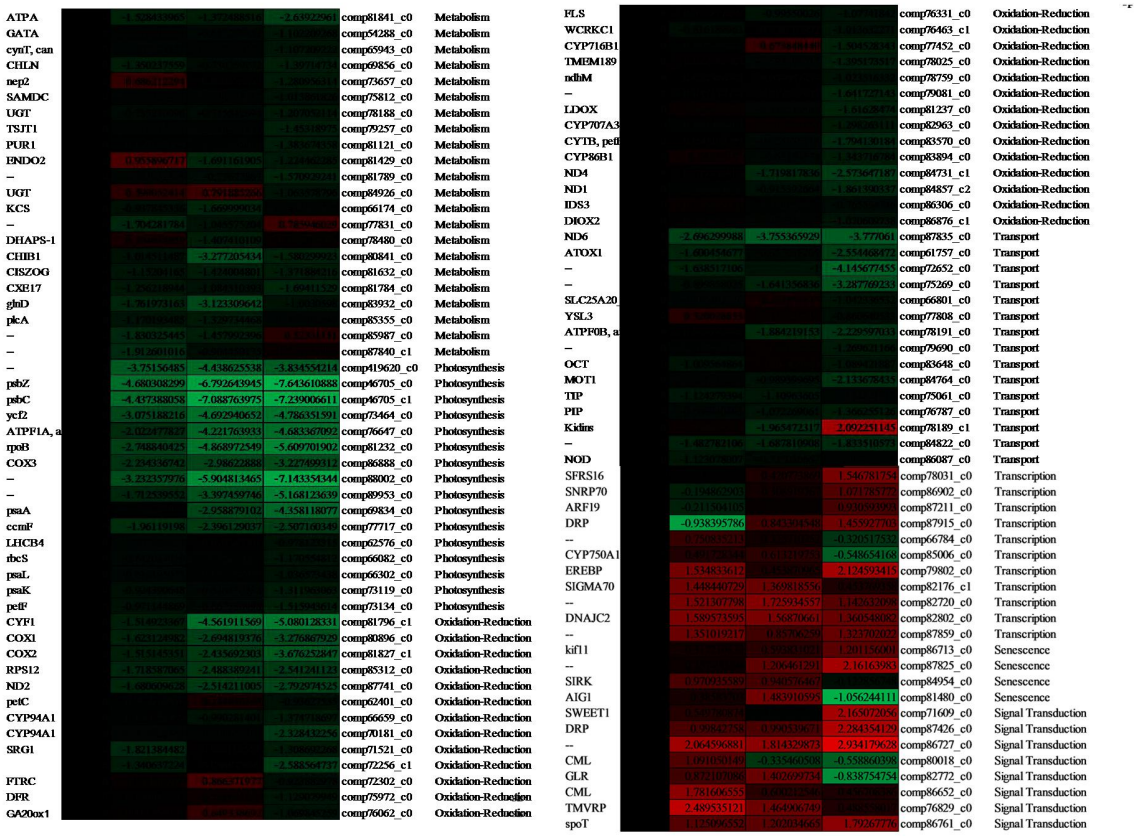

803

804

805

PeerJ Preprints | https://doi.org/10.7287/peerj.preprints.2866v1 | CC BY 4.0 Open Access | rec: 10 Mar 2017, publ: 10 Mar 2017

806 **Fig. 10. Expression patterns of photosynthesis-related unigenes in *Platycladus orientalis***
807 **leaves.**

808 Verification of eight selected DEGs by qRT-PCR. The red column contains the results from
809 qRT-PCR and the blue column contains the results from RNA-seq. *αTUB* was used as the
810 internal control. Both methods show similar gene expression trends. Three biological
811 replicates were performed.

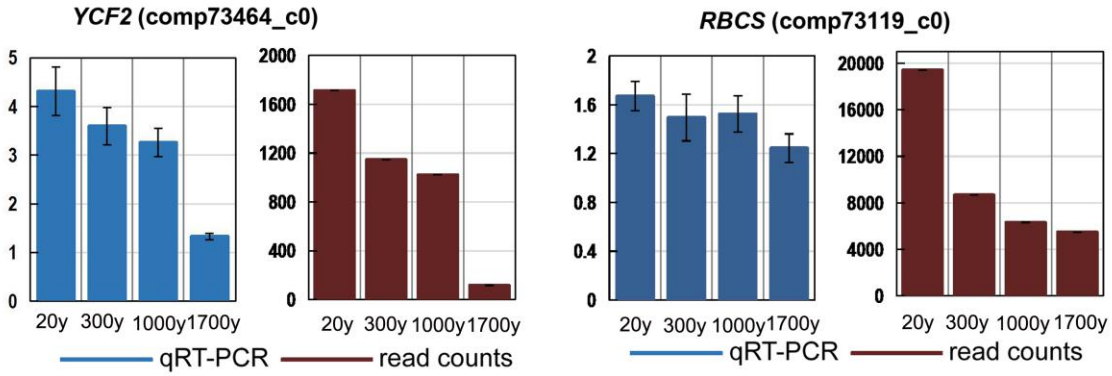

812

813

PeerJ Preprints | https://doi.org/10.7287/peerj.preprints.2866v1 | CC BY 4.0 Open Access | rec: 10 Mar 2017, publ: 10 Mar 2017

Fig. 11. Chlorophyll a, chlorophyll b, and total chlorophyll content.

Vertical bars represent the mean ± SD of four separate experiments. Data were analyzed by ANOVA in the SPASS software.

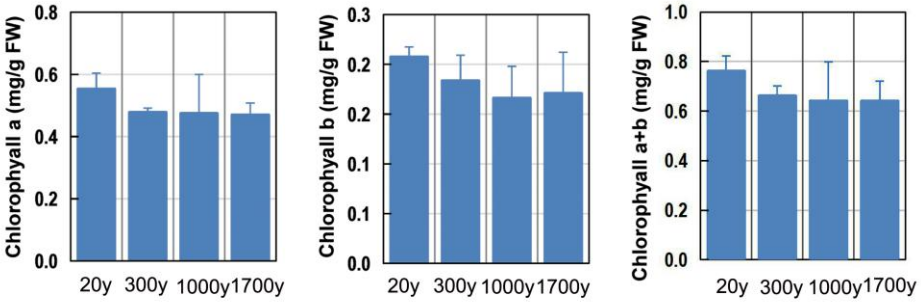

PeerJ Preprints | https://doi.org/10.7287/peerj.preprints.2866v1 | CC BY 4.0 Open Access | rec: 10 Mar 2017, publ: 10 Mar 2017

820

821 **Table Captions**

822 **Table 1. Functional annotation of the *Platycladus orientalis* transcriptome.**

823

Annotated databases	Number of Unigenes	Percentage (%)
Annotated in NR	24080	50.12
Annotated in NT	8380	17.44
Annotated in KO	7783	16.19
Annotated in SwissProt	18483	38.47
Annotated in PFAM	18546	38.6
Annotated in GO	20029	41.68
Annotated in KOG	9877	20.55
Annotated in all Databases	3105	6.46
Annotated in at least one Database	26226	54.58
Total Unigenes	48044	100

824

PeerJ Preprints | https://doi.org/10.7287/peerj.preprints.2866v1 | CC BY 4.0 Open Access | rec: 10 Mar 2017, publ: 10 Mar 2017